

Phase and Thermal Driven Transport across T-Shaped Double Quantum Dot Josephson Junction

Bhupendra Kumar ^{*}, Sachin Verma [†] and Ajay [‡]

Department of Physics, Indian Institute of Technology, Roorkee, 247667, Uttarakhand, India

December 2, 2022

The phase and thermal driven transport properties of the T-shaped uncorrelated double quantum dot Josephson junction are analyzed by using Keldysh non-equilibrium Green's function equation of motion technique. In this setup, we have shown that the side-attached quantum dot provides an additional route for electron transmission which is affecting the transport properties by adjusting the interdot hopping between the main dot and the side dot. We began with investigating the impact of interdot hopping on Andreev bound states and Josephson supercurrent. When a small thermal bias is applied across the superconducting leads, the system exhibits a finite thermal response which is primarily due to the, thermally induced, quasi-particle current. The behavior of the Josephson supercurrent and the quasi-particle current flowing through the quantum dots is examined for various interdot hopping and thermal biasing. Finally, the system is considered in an open circuit configuration where the thermally driven quasi-particle current is compensated by the phase-driven Josephson supercurrent and the thermophase effect is observed. The effect of interdot hopping and the position of quantum dot energy level on the thermophase Seebeck coefficient is investigated.

Keywords: Quantum dots, T-shaped Josephson junction, thermophase Seebeck effect

Introduction

A quantum dot (QD)-based Josephson junction is made up of two Bardeen-Cooper-Schrieffer (BCS) superconducting leads separated by a quantum dot. A DC Josephson supercurrent can flow across the junction without applying potential difference, as the Josephson supercurrent largely depends on the phase difference between the superconductors [1, 2]. Quantum dots have discrete energy levels and can be controlled by tuning their gate voltage or by changing the size of quantum dot [3, 4]. Single-electron (quasi-particle) tunneling and cooper pair tunneling are responsible for charge transport in quantum dot-based Josephson junctions. Charge transport in these single quantum dot-based Josephson junctions have been studied extensively both theoretically [5, 6, 7, 8, 9, 10, 11, 12, 13] as well as experimentally [14, 15, 16, 17, 18, 19, 20, 21]. Using quantum dots allow one to control the current flowing through Josephson junctions. Further, various authors have explored the charge transport properties of double quantum dot Josephson junctions. In such junctions, the double quantum dots are coupled with superconducting leads in series, parallel, and T-shaped geometry [22, 23, 24, 25, 26, 27, 28, 29]. References [30, 31, 32] provides recent detailed reviews on the charge transport properties of single and double quantum dot based Josephson junctions.

On the other hand, due to the limited temperature range, the thermal transport properties of the ordinary S-I-S Josephson junction and quantum dot-based junctions have not been widely explored. Despite this limitation, the thermal transport properties of Josephson junctions are recently attracting great attention [33, 34, 35, 36, 37, 38, 39]. Recently, very few studies have been conducted on the thermal transport properties of quantum dot-based Josephson junctions i.e when both the leads are superconducting [40, 41]. Further, the thermoelectric transport properties of systems where the quantum dot is coupled

*bhupendra_k@ph.iitr.ac.in

†sverma2@ph.iitr.ac.in

‡ajay@ph.iitr.ac.in

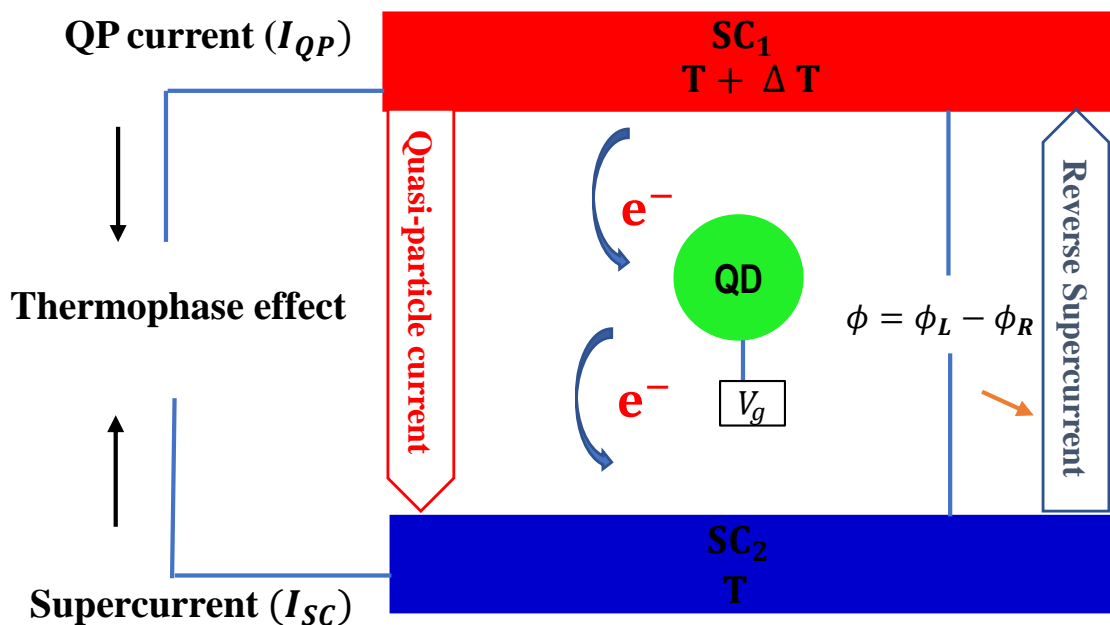


Figure 1: Schematic diagram showing the origin of thermophase Seebeck effect. The cancellation of quasi-particle current, induced by the temperature difference, by phase-driven reverse supercurrent is the origin of thermophase.

between a normal metal and BCS superconductor (N-QD-S) [42, 43, 44] and ferromagnet and BCS superconductor (F-QD-S) [45, 46, 47, 48] have been studied recently. Further, the thermoelectric transport properties of multi-dot and multi-terminal systems with one superconducting lead are also gaining attention [49, 50, 51, 52, 53].

Phase and thermal-driven transport properties of quantum dot-based Josephson junctions can be analyzed through a combination of three currents: quasi-particle current, interference current, and pair current [33, 40, 54]. A thermal gradient induces the quasi-particle current to flow across the junction. Quasi-particle is the only current that contributes to thermal transport in the S-QD-S system. The interference current, which is due to coupling between quasi-particle and condensate shows no contribution to thermal transport and will be ignored in the present study. The pair current or Josephson supercurrent flows across the junction in absence of voltage difference or temperature difference between the superconducting leads. This Josephson current depends on the phase difference between the superconducting leads. In reference, [40, 41] author demonstrates that quantum dot-based Josephson junction shows a significant thermal response on applying the thermal biasing across the superconducting leads. By applying the thermal biasing across the superconducting leads, there appears to be a phase gradient across the superconductors. Therefore, a supercurrent will flow across the junction and it will counterbalance the thermally induced quasi-particle current. This is the open circuit configuration for S-QD-S system i.e. total current $I_C = 0$. The cancellation of quasi-particle current by reverse supercurrent is the origin of concept of thermophase Seebeck effect in quantum dot-based Josephson junctions as shown by the schematic diagram in figure 1.

In the present work, we provide a study of the low-temperature phase and thermal-driven transport properties of a system where uncorrelated double quantum dots are coupled with two superconducting leads in T-shaped geometry (figure 2). In this configuration the main quantum dot (QD_1) is directly coupled with the leads and the side quantum dot (QD_2) is coupled with the main dot but not with the superconducting leads. To study the thermal transport properties of a T-shaped double quantum dot Josephson junction, we have employed Keldysh non-equilibrium Green's equation of motion technique [55, 56]. First, we have studied the interdot hopping dependence of Andreev Bound States (ABS) and supercurrent. Next, total current (which is the combination of quasi-particle current and Josephson supercurrent) is calculated for different temperature differences ΔT and interdot hopping (t). Finally, the thermophase Seebeck coefficient (TPSC) for the T-shaped double quantum dot Josephson junction is analyzed. Since, both the leads are superconductors, so we have taken into

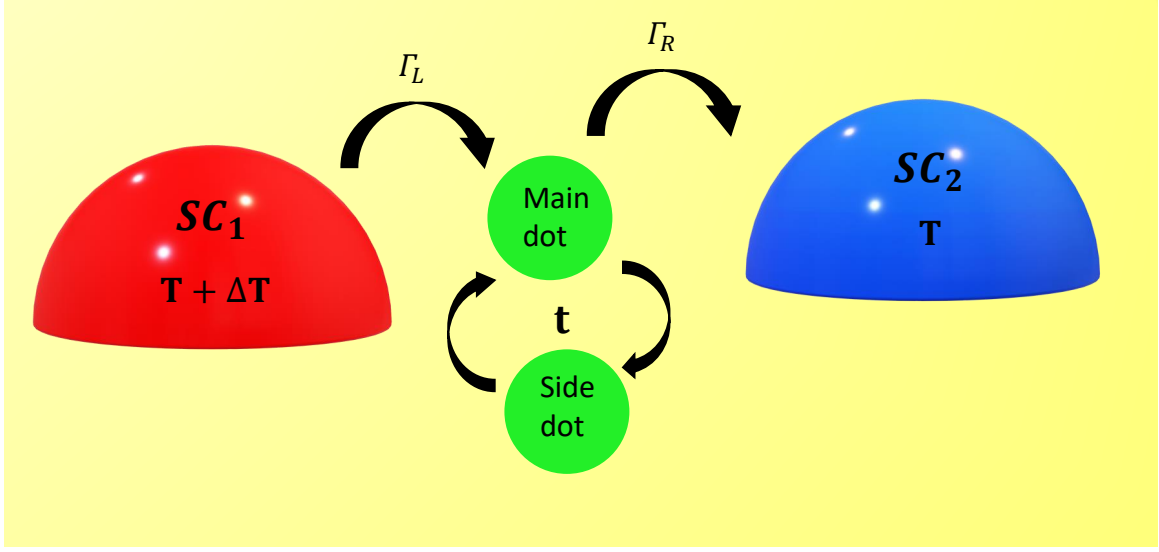


Figure 2: Schematic diagram for double quantum dot in T-shaped geometry coupled with superconducting leads. Main dot (QD_1) is directly coupled with superconducting leads while the side dot (QD_2) is only coupled with the main dot.

account the temperature dependence of the superconducting gap (Δ_α) having a background temperature always less than the superconducting critical temperature T_c .

This paper can be read in the following order: in the preceding section 2, we provide a detailed description of model Hamiltonian and theoretical formalism. Section 3, discusses numerical results. Lastly, section 4 concludes the present work.

2 THEORETICAL FORMULATION

To calculate the transport properties of the T-shaped double quantum dot Josephson junction, we use the generalized Anderson + BCS Hamiltonian in second quantization formalism.

$$\hat{H} = \hat{H}_{leads} + \hat{H}_{QD} + \hat{H}_{tunnel} + \hat{H}_{interdot-hopping} \quad (1)$$

where

$$\begin{aligned} \hat{H}_{leads} &= \sum_{k\sigma,\alpha} \epsilon_{k\alpha} c_{k\sigma,\alpha}^\dagger c_{k\sigma,\alpha} - \left(\sum_{k\alpha} \Delta_\alpha c_{k\uparrow,\alpha}^\dagger c_{-k\downarrow,\alpha}^\dagger + h.c \right) \\ \hat{H}_{QD} &= \sum_{i=1}^{i=2} \sum_{\sigma} \epsilon_{d_{i\sigma}} d_{i\sigma}^\dagger d_{i\sigma} \\ \hat{H}_{tunnel} &= \sum_{k\sigma,\alpha} V_{k,\alpha} c_{k\sigma,\alpha}^\dagger d_{1\sigma} + h.c \\ \hat{H}_{interdot-hopping} &= \sum_{\sigma} t (d_{1\sigma}^\dagger d_{2\sigma} + h.c) \end{aligned}$$

where h.c stands for Hermitian conjugate.

\hat{H}_{leads} is the Hamiltonian for left and right superconducting leads ($\alpha \in L, R$). The first term, describes the free electrons in the superconducting leads; $c_{k\sigma,\alpha}^\dagger (c_{k\sigma,\alpha})$ is the creation (annihilation) operator of electron with spin σ and wave vector \vec{k}

and energy $\epsilon_{k,\alpha}$. The second term in \hat{H}_{leads} is the BCS term and gives the information about the interaction between Cooper pair with temperature dependent superconducting energy gap which is given by [41]

$$\Delta_\alpha(T_\alpha) = \Delta_0 \tanh \left\{ 1.74 \sqrt{\left(\frac{k_B T_c}{k_B T_\alpha} - 1 \right)} \right\} \quad (2)$$

where $\Delta_0 = |\Delta_0|e^{i\phi_\alpha}$ is the superconducting gap at absolute zero temperature with ϕ_α as the phase of superconducting leads, T_c is superconducting critical temperature, T_α is the temperature of superconducting leads and k_B is the Boltzman constant.

\hat{H}_{QD} is the Hamiltonian for main dot (QD_1) and side dot (QD_2). QD_1 ($i=1$) and QD_2 ($i=2$) has energy $\epsilon_{d_{i\sigma}}$ with $d_{i\sigma}^\dagger$ ($d_{i\sigma}$) as the fermionic creation operator (annihilation operator) of electrons with spin σ and $n_{d_{i\sigma}} = d_{i\sigma}^\dagger d_{i\sigma}$ is the number operator. We have neglected the onsite Coulomb interaction U_i for simplification.

\hat{H}_{tunnel} is tunneling Hamiltonian between the energy level of the main dot and superconducting leads with interaction strength V_{k_1}, α . Further, we have consider the symmetric coupling strength of QD_1 to the left and right leads i.e. $V_{k_1;L}=V_{k_1;R}$.

The last term $\hat{H}_{interdot-hopping}$ describes the interaction of electrons of two quantum dots via a hopping like term of strength t . Note that, there is no direct interaction between superconducting leads and QD_2 .

Bogoliubov transformation is used to diagonalize the BCS part of the Hamiltonian. For this, we introduce a new fermionic quasiparticle operator β with coefficient u_k and v_k which satisfies the normalization condition $|u_k|^2 + |v_k|^2 = 1$

$$c_{k\uparrow} = u_k^* \beta_{k\uparrow} + v_k \beta_{-k\downarrow}^\dagger \quad (3)$$

$$c_{-k\downarrow}^\dagger = u_k \beta_{-k\downarrow}^\dagger - v_k^* \beta_{k\uparrow} \quad (4)$$

By replacing the fermionic operator $c_{k\uparrow}$ and $c_{-k\downarrow}^\dagger$ with new quasi-particle operator, we get the effective Hamiltonian

$$\begin{aligned} \hat{H} = & \sum_{k\alpha} E_{k\alpha} (\beta_{k\uparrow,\alpha}^\dagger \beta_{k\uparrow,\alpha} + \beta_{-k\downarrow,\alpha}^\dagger \beta_{-k\downarrow,\alpha}) \\ & + \sum_{k\alpha} (V_{k\alpha} u_k^* \beta_{k\uparrow,\alpha}^\dagger d_{1\uparrow} + V_{k\alpha} u_k^* \beta_{-k\downarrow,\alpha}^\dagger d_{1\downarrow}) \\ & + \sum_{k\alpha} (V_{k\alpha}^* u_k d_{1\uparrow}^\dagger \beta_{k\uparrow,\alpha} + V_{k\alpha}^* u_k d_{1\downarrow}^\dagger \beta_{-k\downarrow,\alpha}) \\ & + \sum_{k\alpha} V_{k\alpha} v_k (\beta_{-k\downarrow,\alpha} d_{1\uparrow} - \beta_{k\uparrow,\alpha} d_{1\downarrow}) \\ & + \sum_{k\alpha} V_{k\alpha}^* v_k^* (d_{1\uparrow}^\dagger \beta_{-k\downarrow,\alpha}^\dagger - d_{1\downarrow}^\dagger \beta_{k\uparrow,\alpha}^\dagger) \\ & + \epsilon_{d_1} (d_{1\uparrow}^\dagger d_{1\uparrow} + d_{1\downarrow}^\dagger d_{1\downarrow}) \\ & + \epsilon_{d_2} (d_{2\uparrow}^\dagger d_{2\uparrow} + d_{2\downarrow}^\dagger d_{2\downarrow}) \\ & + t (d_{1\uparrow}^\dagger d_{2\uparrow} + d_{1\downarrow}^\dagger d_{2\downarrow} + d_{2\uparrow}^\dagger d_{1\uparrow} + d_{2\downarrow}^\dagger d_{1\downarrow}) \end{aligned} \quad (5)$$

where $E_{k\alpha} = \sqrt{\epsilon_{k\alpha}^2 + |\Delta_\alpha|^2}$ is excitation quasi-particle energy of the superconducting leads. The coefficients u_k and v_k can be expressed as

$$|u_k|^2 = \frac{1}{2} \left(1 + \frac{\epsilon_{k,\alpha}}{\sqrt{\epsilon_{k,\alpha}^2 + |\Delta_\alpha|^2}} \right) \quad (6)$$

$$|v_k|^2 = \frac{1}{2} \left(1 - \frac{\epsilon_{k,\alpha}}{\sqrt{\epsilon_{k,\alpha}^2 + |\Delta_\alpha|^2}} \right) \quad (7)$$

We have used Green's equation of motion method (EOM) to solve the above effective Hamiltonian (Eq. 5). To calculate the spectral and transport properties of T-shaped double quantum dot Josephson junction system, we need single-particle retarded Green's function of main quantum dot QD_1 which is defined in Zubarev notation [55, 56, 57]

$$\langle\langle d_\sigma(t); d_\sigma^\dagger(0) \rangle\rangle = -i\theta(t)\langle[d_\sigma(t), d_\sigma^\dagger(0)]_+\rangle$$

The Fourier transform of the above retarded Green's function should satisfy the following equation of motion

$$\omega\langle\langle d_\sigma | d_\sigma^\dagger \rangle\rangle_\omega = \langle\{d_\sigma, d_\sigma^\dagger\}_+\rangle + \langle\langle [d_\sigma, H]_- | d_\sigma^\dagger \rangle\rangle_\omega \quad (8)$$

In Nimbu space, Green's function of the main quantum dot can be represented by a 2×2 matrix:

$$\mathbf{G}^r(\omega) = \begin{pmatrix} G_{11}^r(\omega) & G_{12}^r(\omega) \\ G_{21}^r(\omega) & G_{22}^r(\omega) \end{pmatrix} = \begin{pmatrix} \langle\langle d_{1\uparrow} | d_{1\uparrow}^\dagger \rangle\rangle & \langle\langle d_{1\downarrow} | d_{1\uparrow}^\dagger \rangle\rangle \\ \langle\langle d_{1\downarrow}^\dagger | d_{1\uparrow}^\dagger \rangle\rangle & \langle\langle d_{1\downarrow}^\dagger | d_{1\downarrow} \rangle\rangle \end{pmatrix} \quad (9)$$

By using Green's function EOM technique (Eq. 8), we obtain the following coupled equations for QD_1

$$\begin{aligned} (\omega - \epsilon_{d_1})\langle\langle d_{1\uparrow} | d_{1\uparrow}^\dagger \rangle\rangle &= 1 + \sum_{k\alpha} V_{k\alpha} u_k^* \langle\langle \beta_{k\uparrow, \alpha} | d_{1\uparrow}^\dagger \rangle\rangle \\ &+ \sum_{k\alpha} V_{k\alpha} v_k \langle\langle \beta_{-k\downarrow, \alpha}^\dagger | d_{1\uparrow}^\dagger \rangle\rangle \\ &+ t\langle\langle d_{2\uparrow} | d_{1\uparrow}^\dagger \rangle\rangle \end{aligned} \quad (10)$$

$$\begin{aligned} (\omega - E_{k\alpha})\langle\langle \beta_{k\uparrow, \alpha} | d_{1\uparrow}^\dagger \rangle\rangle &= \sum_{k\alpha} V_{k\alpha}^* u_k \langle\langle d_{1\uparrow} | d_{1\uparrow}^\dagger \rangle\rangle \\ &+ \sum_{k\alpha} V_{k\alpha} v_k \langle\langle d_{1\downarrow}^\dagger | d_{1\uparrow}^\dagger \rangle\rangle \end{aligned} \quad (11)$$

$$\begin{aligned} (\omega + E_{k\alpha})\langle\langle \beta_{-k\downarrow, \alpha}^\dagger | d_{1\uparrow}^\dagger \rangle\rangle &= \sum_{k\alpha} V_{k\alpha}^* v_k^* \langle\langle d_{1\uparrow} | d_{1\uparrow}^\dagger \rangle\rangle \\ &- \sum_{k\alpha} V_{k\alpha} u_k^* \langle\langle d_{1\downarrow}^\dagger | d_{1\uparrow}^\dagger \rangle\rangle \end{aligned} \quad (12)$$

$$\begin{aligned} (\omega + \epsilon_{d_1})\langle\langle d_{1\downarrow}^\dagger | d_{1\uparrow}^\dagger \rangle\rangle &= \sum_{k\alpha} V_{k\alpha}^* v_k^* \langle\langle \beta_{k\uparrow, \alpha} | d_{1\uparrow}^\dagger \rangle\rangle \\ &+ \sum_{k\alpha} V_{k\alpha}^* u_k \langle\langle \beta_{-k\downarrow, \alpha}^\dagger | d_{1\uparrow}^\dagger \rangle\rangle \\ &- t\langle\langle d_{2\downarrow}^\dagger | d_{1\uparrow}^\dagger \rangle\rangle \end{aligned} \quad (13)$$

$$(\omega - \epsilon_{d_2})\langle\langle d_{2\uparrow} | d_{1\uparrow}^\dagger \rangle\rangle = t\langle\langle d_{1\uparrow} | d_{1\uparrow}^\dagger \rangle\rangle \quad (14)$$

$$(\omega - \epsilon_{d_2})\langle\langle d_{2\downarrow}^\dagger | d_{1\uparrow}^\dagger \rangle\rangle = -t\langle\langle d_{1\downarrow}^\dagger | d_{1\uparrow}^\dagger \rangle\rangle \quad (15)$$

After solving these closed set of coupled equations (Eq. 10-15) the expression for single particle retarded Green's function of the main dot with spin $\sigma = \uparrow$ can be written as:

$$G_{11}^r(\omega) = \langle\langle d_{1\uparrow} | d_{1\uparrow}^\dagger \rangle\rangle = \frac{\omega + \epsilon_{d_1} - \frac{t^2}{\omega + \epsilon_{d_2}} - I_1}{(\omega + \epsilon_{d_1} - \frac{t^2}{\omega + \epsilon_{d_2}} - I_1)(\omega - \epsilon_{d_1} - \frac{t^2}{\omega - \epsilon_{d_2}} - I_2) - (I_3)^2} \quad (16)$$

In above Green's function (Eq. 16) I_1 , I_2 are the diagonal, and I_3 is the off-diagonal part of self-energy, which corresponds to the induced pairing, due to the coupling between the quantum dot and superconducting leads.

The expressions for I_1 , I_2 and I_3 are

$$I_1 = \sum_{k\alpha} |V_{k\alpha}|^2 \left(\frac{|u_k|^2}{\omega + E_{k\alpha}} + \frac{|v_k|^2}{\omega - E_{k\alpha}} \right) \quad (17)$$

$$I_2 = \sum_{k\alpha} |V_{k\alpha}|^2 \left(\frac{|u_k|^2}{\omega - E_{k\alpha}} + \frac{|v_k|^2}{\omega + E_{k\alpha}} \right) \quad (18)$$

$$I_3 = \sum_{k\alpha} |V_{k\alpha}|^2 u_k v_k^* \left(\frac{1}{\omega - E_{k\alpha}} - \frac{1}{\omega + E_{k\alpha}} \right) \quad (19)$$

Transforming the summation into integration and by defining the tunneling rate $\Gamma_\alpha = 2\pi\rho_0|V_{k\alpha}|^2$ where ρ_0 is the density of states in normal metallic state, we obtained the following expressions for I_1 , I_2 and I_3 :

$$I_1 = I_2 = - \sum_{\alpha \in L, R} \left(\frac{\Gamma_\alpha \omega}{\sqrt{\Delta_\alpha^2 - \omega^2}} \theta(\Delta - |\omega|) + i \left(\frac{\Gamma_\alpha \omega}{\sqrt{\omega^2 - \Delta_\alpha^2}} \theta(|\omega| - \Delta) \right) \right) \quad (20)$$

$$I_3 = - \sum_{\alpha \in L, R} \left(\frac{\Gamma_\alpha \Delta_\alpha}{\sqrt{\Delta_\alpha^2 - \omega^2}} \theta(\Delta - |\omega|) + i \left(\frac{\Gamma_\alpha \Delta_\alpha}{\sqrt{\omega^2 - \Delta_\alpha^2}} \theta(|\omega| - \Delta) \right) \right) \quad (21)$$

Similarly, the off-diagonal Green's function $G^r_{21}(\omega)$ can be calculated with the help of coupled equations (10-15).

$$G^r_{21}(\omega) = \langle\langle d_{1\downarrow}^\dagger | d_{1\uparrow}^\dagger \rangle\rangle = \frac{I_3}{[(\omega + \epsilon_{d_{1\downarrow}} - \frac{t^2}{\omega + \epsilon_{d_{2\downarrow}}} + I_1)(\omega - \epsilon_{d_{1\uparrow}} - \frac{t^2}{\omega - \epsilon_{d_{2\uparrow}}} + I_2) - (I_3)^2]} \quad (22)$$

Other Green's function can be obtained with the help of the following relations:

$$G^r_{22}(\omega) = -G^r_{11}(-\omega)^* \quad (23)$$

$$G^r_{12}(\omega) = G^r_{21}(-\omega)^*$$

By equating the denominator of single particle retarded Green's function G^r_{11} (Eq. 16) equal to zero, the energies of Andreev Bound States (ABS) can be analyzed which is discussed in section III.

As discussed in section 1, for quantum dot-based Josephson junction, we can distribute the charge current in three parts [33, 40]:

$$I_C = I_{QP}(\epsilon_{di}, \phi, T, \Delta T) + I_{pair-QP}(\epsilon_{di}, \phi, T, \Delta T) \cos^2 \frac{\phi}{2} + I_{SC}(\epsilon_{di}, \phi, T, \Delta T) \quad (24)$$

The first term is quasi-particle current and is responsible for thermal transport in this system. The second term has no contribution to thermal transport and can be neglected here. The third term in current is due to cooper pair tunneling and is responsible for the supercurrent in the system. Here, we present the full derivation of Josephson supercurrent and quasi-particle current. For the current expression, we follow the formulation given in reference [9, 55, 58]. The retarded Green's function \mathbf{G}^r (Eq. 9) of main quantum dot can also be written as:

$$\mathbf{G}^r = [\mathbf{g}^{r^{-1}} - \mathbf{\Sigma}^r]^{-1} = \frac{1}{A(\omega)} \begin{pmatrix} \mathbf{g}^r_{22}(\omega) - \mathbf{\Sigma}^r_{22} & \mathbf{\Sigma}^r_{12} \\ \mathbf{\Sigma}^r_{21} & \mathbf{g}^r_{11}(\omega) - \mathbf{\Sigma}^r_{11} \end{pmatrix} \quad (25)$$

Where \mathbf{G}^r is Green's function of the main quantum dot with leads and \mathbf{g}^r is Green's function of the main quantum dot without leads. $\mathbf{\Sigma}^r = \mathbf{\Sigma}_L^r + \mathbf{\Sigma}_R^r$ is the retarded self-energy due to coupling between the main quantum dot and superconducting leads. $A(\omega)$ is the denominator of Green's function and is defined as

$$A(\omega) = \det[\mathbf{g}^{r^{-1}} - \mathbf{\Sigma}^r] \quad (26)$$

From Eq's. (9,16,22,23), \mathbf{g}^r for T-shaped double quantum dot Josephson junction, can be written as

$$\mathbf{g}^{r^{-1}} = \begin{pmatrix} \omega - \epsilon_{d_1} - \frac{t^2}{\omega - \epsilon_{d_1}} + i0^+ & 0 \\ 0 & \omega + \epsilon_{d_1} - \frac{t^2}{\omega + \epsilon_{d_1}} + i0^+ \end{pmatrix} \quad (27)$$

The retarded self-energy ($\mathbf{\Sigma}_\alpha^r$) of α lead is defined as

$$\mathbf{\Sigma}_\alpha^r(\omega) = -\frac{i}{2}\Gamma_\alpha\rho(\omega) \begin{pmatrix} 1 & -\frac{\Delta}{\omega}e^{-i\phi_\alpha} \\ -\frac{\Delta}{\omega}e^{i\phi_\alpha} & 1 \end{pmatrix} \quad (28)$$

For simplicity, we assumed that both superconductors are identical and have a finite phase difference, $\Gamma_\alpha = \Gamma_L = \Gamma_R = \Gamma$, and $\Delta_\alpha = \Delta_L = \Delta_R = \Delta$

$$\mathbf{\Sigma}^r = \mathbf{\Sigma}_L^r + \mathbf{\Sigma}_R^r = -i\Gamma\rho(\omega) \begin{pmatrix} 1 & -\frac{\Delta}{\omega}\cos\frac{\phi}{2} \\ -\frac{\Delta}{\omega}\cos\frac{\phi}{2} & 1 \end{pmatrix} \quad (29)$$

$$\tilde{\mathbf{\Sigma}}^r = \mathbf{\Sigma}_L^r - \mathbf{\Sigma}_R^r = -i\Gamma\rho(\omega) \begin{pmatrix} 0 & -\frac{\Delta}{\omega}(-i)\sin\frac{\phi}{2} \\ -\frac{\Delta}{\omega}(i)\sin\frac{\phi}{2} & 0 \end{pmatrix} \quad (30)$$

where Γ is the symmetric coupling strength between the main quantum dot and superconducting leads. $\rho(\omega)$ is the modified density of state of the superconductor and can be defined as

$$\rho(\omega) = \begin{cases} \frac{|\omega|}{\sqrt{\omega^2 - \Delta^2}}, & |\omega| > \Delta \\ \frac{|\omega|}{i\sqrt{\Delta^2 - \omega^2}}, & |\omega| < \Delta \end{cases} \quad (31)$$

By taking the current conservation condition $I_L + I_R = 0$, the general formula of Josephson supercurrent for the superconductor-quantum dot systems can be written as [9]:

$$I_{SC} = \frac{1}{2}(I_L - I_R) = \frac{e}{h} \int d\omega \text{Re}[\mathbf{G}\tilde{\mathbf{\Sigma}}]_{11-22}^< \quad (32)$$

Where \mathbf{G} and $\mathbf{\Sigma}_\alpha$ are 2×2 Fourier transformed Nambu matrices.

By using the Langreth relation we can write [55];

$$\text{Re}[\mathbf{G}\tilde{\mathbf{\Sigma}}]_{11-22}^< = \text{Re}[\mathbf{G}^<\tilde{\mathbf{\Sigma}}^a + \mathbf{G}^r\tilde{\mathbf{\Sigma}}^<]_{11} - \text{Re}[\mathbf{G}^<\tilde{\mathbf{\Sigma}}^a + \mathbf{G}^r\tilde{\mathbf{\Sigma}}^<]_{22} \quad (33)$$

with $(\mathbf{G}^r)^\dagger = \mathbf{G}^a$, $(\tilde{\mathbf{\Sigma}}^r)^\dagger = \tilde{\mathbf{\Sigma}}^a$

On applying the fluctuation-dissipation theorem, we can define: $\mathbf{G}^< = f(\omega)[\mathbf{G}^a - \mathbf{G}^r]$ and $\tilde{\mathbf{\Sigma}}^< = f(\omega)[\tilde{\mathbf{\Sigma}}^a - \tilde{\mathbf{\Sigma}}^r]$, where $f(\omega) = \frac{1}{e^{\omega/k_B T} + 1}$ is Fermi distribution function and \mathbf{G}^a , $\mathbf{G}^<$ are advanced and lesser Green's function respectively.

Substituting the above relations in Eq. (33) and using Eq. (25) and Eq. (30)

$$\text{Re}[\mathbf{G}\tilde{\mathbf{\Sigma}}^r]_{11-22}^< = f(\omega)\text{Re}[(\tilde{\mathbf{\Sigma}}^r\mathbf{G}^r)^\dagger - \mathbf{G}^r\tilde{\mathbf{\Sigma}}^r]_{11} - f(\omega)\text{Re}[(\tilde{\mathbf{\Sigma}}^r\mathbf{G}^r)^\dagger - \mathbf{G}^r\tilde{\mathbf{\Sigma}}^r]_{22} \quad (34)$$

$$(\tilde{\Sigma}^r \mathbf{G}^r)_{11}^\dagger = \frac{1}{A(\omega)} \begin{pmatrix} 0 & -\frac{\Delta}{\omega}(-i)\sin\frac{\phi}{2} \\ -\frac{\Delta}{\omega}(i)\sin\frac{\phi}{2} & 0 \end{pmatrix} \begin{pmatrix} \mathbf{g}_{22}^r(\omega) - \Sigma_{22}^r & \Sigma_{12}^r \\ \Sigma_{21}^r & \mathbf{g}_{11}^r(\omega) - \Sigma_{11}^r \end{pmatrix} \quad (35)$$

Similarly, we obtain the $(\mathbf{G}^r \tilde{\Sigma}^r)_{11}$ and the $Re[(\tilde{\Sigma}^r \mathbf{G}^r)^\dagger - \mathbf{G}^r \tilde{\Sigma}^r]_{22}$ in Eq. (34). Finally it can be written as:

$$Re[\mathbf{G} \tilde{\Sigma}]_{11-22}^< = \frac{\Gamma^2 \Delta^2}{\omega^2 - \Delta^2} f(\omega) \sin\phi \text{Im} \left[\frac{-1}{A(\omega)} \right] \quad (36)$$

By substituting Eq. (36) in Eq. (32) and taking both spin up and spin down into consideration, the final expression for Josephson supercurrent can be written as

$$I_{SC} = \frac{2e}{h} \int d\omega \frac{\Gamma^2 \Delta^2}{\omega^2 - \Delta^2} f(\omega) \sin\phi \text{Im} \left[\frac{-1}{A(\omega)} \right] \quad (37)$$

Similar to Josephson supercurrent, we can also derive the expression of quasi-particle current for superconductor-quantum dot systems by following the formalism given in reference [55, 59, 58].

$$I_\alpha = \frac{4ie}{h} \int d\omega \Gamma_\alpha \frac{|\omega|}{\sqrt{\omega^2 - \Delta_\alpha^2}} \{f_\alpha(\omega)[G_{11}^r(\omega) - G_{11}^a(\omega)] + G_{11}^<(\omega)\} \quad (38)$$

By current conservation condition i.e. $I_L + I_R = 0$, the symmetrize form of current can be written as

$$I_{QP} = I_L = -I_R = \frac{1}{2}(I_L - I_R)$$

$$I_{QP} = \frac{2ie}{h} \int d\omega \{[\Gamma_L \frac{|\omega|}{\sqrt{\omega^2 - \Delta_L^2}} f_L(\omega) - \Gamma_R \frac{|\omega|}{\sqrt{\omega^2 - \Delta_R^2}} f_R(\omega)][G_{11}^r(\omega) - G_{11}^a(\omega)] + [\Gamma_L(\omega) - \Gamma_R(\omega)]G_{11}^<(\omega)\} \quad (39)$$

For the symmetric case ($\Gamma_\alpha = \Gamma_L = \Gamma_R = \Gamma$ and $\Delta_\alpha = \Delta_L = \Delta_R = \Delta$) the above equation becomes

$$I_{QP} = \frac{2ie}{h} \int d\omega \Gamma \frac{|\omega|}{\sqrt{\omega^2 - \Delta^2}} \{f_L(\omega) - f_R(\omega)\}[G_{11}^r(\omega) - G_{11}^a(\omega)] \quad (40)$$

where $f_L(\omega) = \frac{1}{e^{\omega/k_B(T+\Delta T)} + 1}$, $f_R(\omega) = \frac{1}{e^{\omega/k_B T} + 1}$ are the Fermi-distribution function of left and right superconducting leads and $[G_{11}^r(\omega) - G_{11}^a(\omega)] = \text{Im}[-G_{11}^r(\omega)]$.

The expression of quasi-particle current for linear response regime (thermal gradient between superconducting leads will be small, $\Delta T \rightarrow 0$) can be simplified by using power series expansion of the Fermi-distribution function of left and right superconducting leads:

$$I_{QP} = \frac{2e}{h} \int d\omega \frac{df(\omega)}{dT} \Gamma \text{Re}(\rho(\omega)) \text{Im}[-G_{11}^r(\omega)] \Delta T \quad (41)$$

In section 1, we have already discussed the origin of the thermophase effect. Within the linear response regime, the thermophase Seebeck coefficient S_ϕ is defined analogous to the thermovoltage Seebeck coefficient and can be simplified using Eq. (24);

$$S_\phi = - \left(\frac{\Delta\phi}{\Delta T} \right)_{I=0} = \frac{dI_{QP}/d\Delta T}{I_{SC}} \quad (42)$$

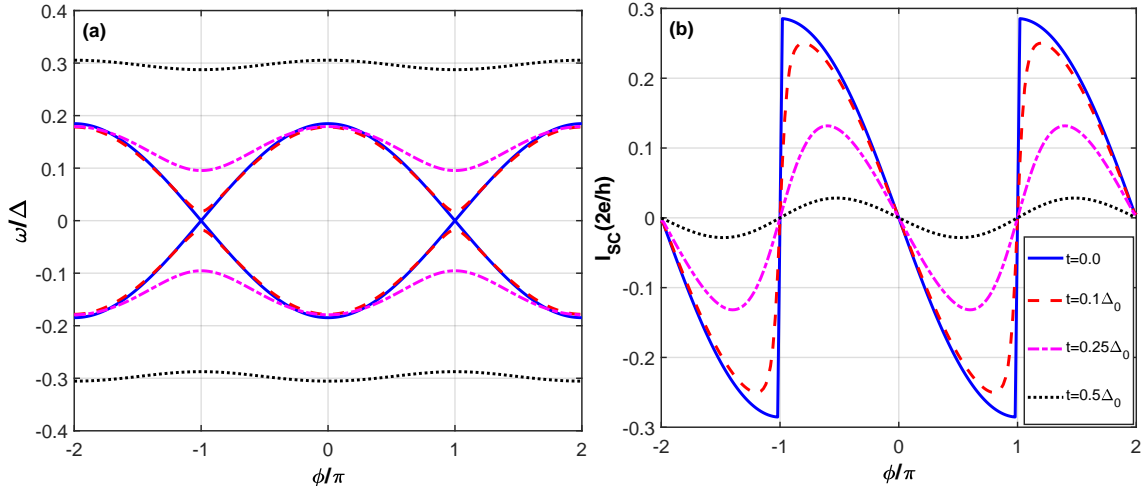


Figure 3: (a) Energy of Andreev bound states and (b) Josephson current as a function of superconducting phase difference (ϕ) for different values of interdot hopping (t) at absolute zero temperature. The other parameters are $\Gamma = 0.1\Delta_0$, $\epsilon_{d_1} = 0$, $\epsilon_{d_2} = 0.5\Delta_0$.

3 RESULTS and DISCUSSION

In this section, we present the numerical results and discussion for the T-shaped double quantum dot Josephson junction. Transport properties are discussed for uncorrelated quantum dots. The superconducting gap at absolute zero temperature (Δ_0) is considered as the energy unit, where Δ_0 is in meV.

In figure 3, we plot the energy of Andreev Bound states (ABS) and Josephson current as a function of superconducting phase difference (ϕ) for different values of interdot hopping (t). First, when QD_2 is decoupled from QD_1 i.e. $t=0$, the system shows the properties of the usual S-QD-S Josephson junction. In this case, the supercurrent is discontinuous at $\phi = \pm\pi$ and upper and lower ABS crosses the Fermi energy ($\omega = 0$). Thus for $t=0$, the system acts as a perfect transmitting channel. When QD_2 is coupled with QD_1 then supercurrent shows sinusoidal behaviour and a finite gap is generated between lower and upper ABS at $\phi = \pm\pi$. Further increasing the value of interdot hopping, this supercurrent is suppressed. This suppression of supercurrent is because coupling QD_1 with the QD_2 , the electrons tends to tunnel into QD_2 . This causes interference destruction between two transport channels and as a result the supercurrent decreases. Thus for $t > 0$, the system does not acts as a perfect transmitting channel. The suppression of supercurrent can also be explained in terms of the splitting of QDs energy level due to interdot hopping. When $t \neq 0$, the equivalent level of QDs splits into two levels i.e. $\bar{\epsilon}_{d_i} = \epsilon_{d_i} \pm t$. The equivalent energy level $\bar{\epsilon}_{d_i}$ moves far away from the Fermi level with increasing interdot hopping and supercurrent decreases.

In figure 4 [(a)-(d)], we plot the total current as a function of superconducting phase difference (ϕ) for several values of thermal biasing (ΔT) and interdot hopping. First, by decoupling QD_2 from QD_1 (Fig 4 a) the results of S-QD-S system are reproduced [40]. When both QD_1 and QD_2 are coupled, then there is suppression in the magnitude of total current with increasing interdot hopping, which is discussed in the previous paragraph. In insets 4(b), the individual behavior of Josephson current and quasi-particle current are shown. It is observed that Josephson current is almost independent of thermal biasing (ΔT) and largely depends on superconducting phase difference (ϕ). On other hand, the quasi-particle current totally depends on the thermal biasing (ΔT). It is important to note that in total current, the sinusoidal nature is due to Josephson current, and the shift in magnitude is due to quasi-particle current. With an increase in interdot hopping, the amplitude of the supercurrent and total current vanishes. In inset 4(d), the behaviour of quasi-particle current is plotted as a function of interdot hopping. It is observed that quasi-particle current first increases with interdot hopping and then attain a maximum value for $k_B T \sim t$, and then decreases with a further increase in the value of interdot hopping.

As discussed previously, the origin of the thermophase effect is due to the vanishing total current in open circuit configuration i.e. thermal-driven quasi-particle current is compensated by the phase-driven Josephson supercurrent flowing in the

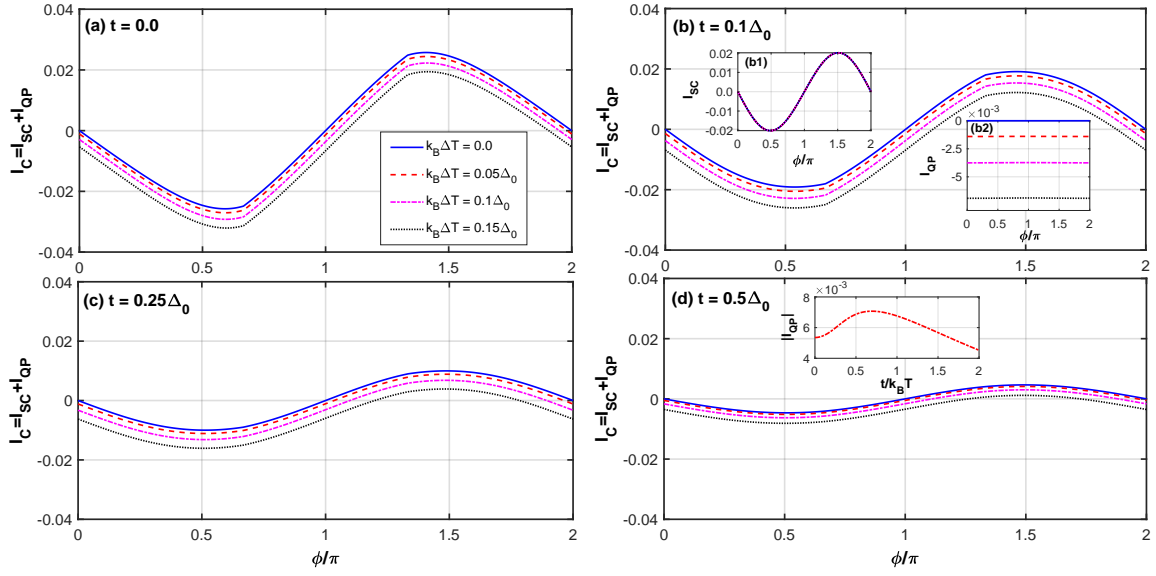


Figure 4: Total current (supercurrent + quasi-particle current) as a function of superconducting phase difference (ϕ) for different interdot hopping (t) and thermal biasing ΔT . Insets (b_1) and (b_2) show the separate behaviour of Josephson current and quasi-particle current with ϕ and ΔT . Inset in figure (d) shows the variation of quasi-particle current as a function of interdot hopping. The other parameters are $\Gamma = 0.1\Delta_0$, $k_B T = 0.2\Delta_0$, $\epsilon_{d_1} = \epsilon_{d_2} = -1.0\Delta_0$.

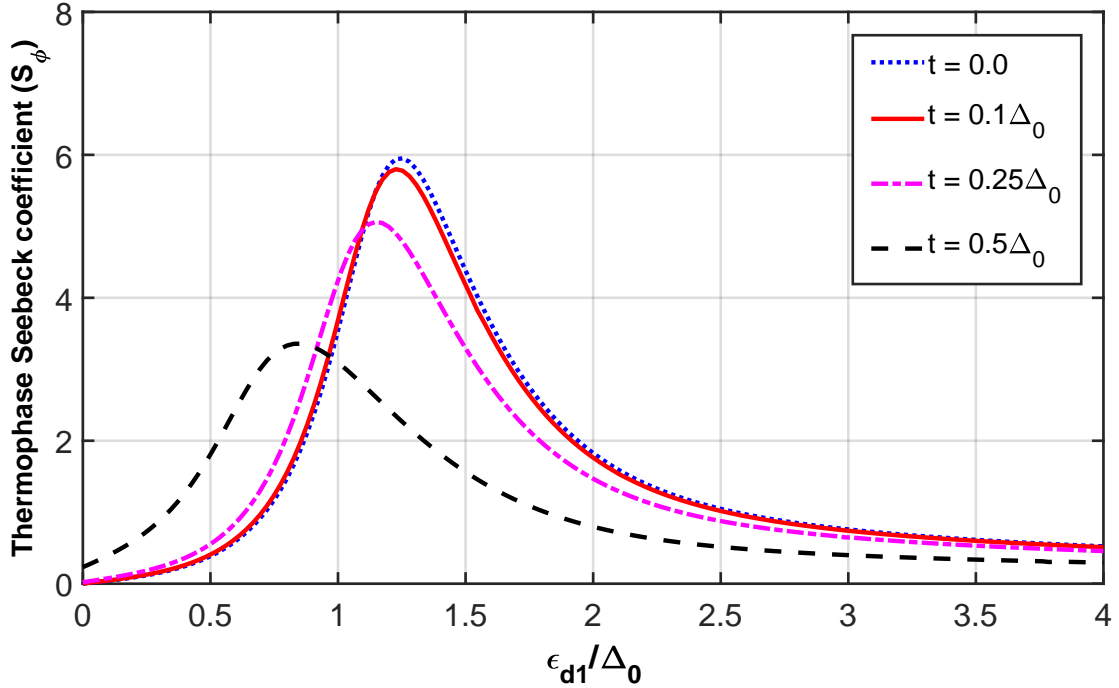


Figure 5: The variation of thermophase Seebeck coefficient (S_ϕ) with QD_1 energy level ϵ_{d_1} for different interdot hopping (t). The other parameters are $\Gamma = 0.1\Delta_0$, $k_B T = 0.2\Delta_0$, $\epsilon_{d_2} = 0.5\Delta_0$.

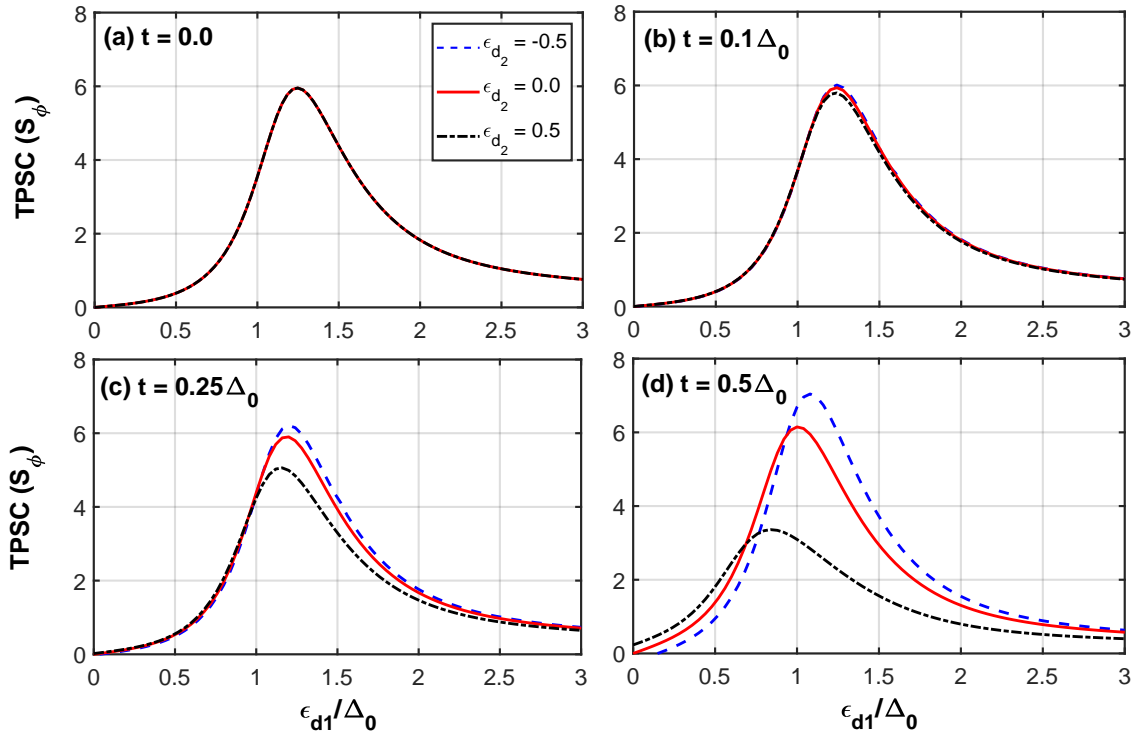


Figure 6: The variation of thermophase Seebeck coefficient (S_ϕ) with QD_1 energy level ϵ_{d_1} for different values of QD_2 energy level ϵ_{d_2} and t . The other parameters are $\Gamma = 0.1\Delta_0$, $k_B T = 0.2\Delta_0$.

reverse direction. In figure 5 and 6, we have analyzed thermophase Seebeck coefficient (S_ϕ) of S-TDQD-S in linear response regime for uncorrelated quantum dots.

In figure 5, we have plotted the thermophase Seebeck coefficient (TPSC) as a function of QD_1 energy level for different interdot hopping. It is observed that TPSC (S_ϕ) peaks are highest for $t=0$ i.e., when QD_2 is decoupled from QD_1 [40]. When QD_2 is coupled with QD_1 , TPSC peaks start decreasing with increasing interdot hopping (t). To achieve a high thermophase peak Josephson current should compensate the quasi-particle current totally. As we have shown that Josephson supercurrent decreases with increasing interdot hopping, therefore it compensates less quasi-particle current. Thus, TPSC peaks decrease and produce a shift in peaks with increasing interdot hopping.

The magnitude of TPSC not only depends on interdot hopping but also depends on the position of QD_2 energy levels whether it lies above or below the Fermi level. In figure 6, we plot the thermophase Seebeck coefficient (S_ϕ) as a function of QD_1 energy level for different values of QD_2 energy level. When QD_2 is decoupled from QD_1 , then system reproduces the results of S-QD-S for TPSC (S_ϕ). For finite interdot hopping, the magnitude of TPSC peaks are enhanced when QD_2 energy level lies below the Fermi level. The enhancement of TPSC peaks can be explained as follows: when QD_2 energy level lies below the Fermi level, the equivalent or effective level lies close to the Fermi level which supports the resonant cooper pair tunneling. Therefore thermally induced quasi-particle is compensated by Josephson supercurrent completely i.e. large magnitude of TPSC peaks. These results for different values of QD_2 energy levels can be directly compared with the TPSC plots as discussed in figure (5).

4 CONCLUSION

We have addressed the phase-driven and thermal-driven transport properties through a T-shaped double quantum dot Josephson junction. For uncorrelated quantum dots, the impact of interdot hopping on Andreev bound states (ABS) and Josephson supercurrent are investigated. For a finite value of interdot hopping, Josephson supercurrent exhibits sinusoidal

nature while ABS shows a finite gap around the Fermi level. The magnitude of Josephson supercurrent decreases with increasing interdot hopping because the electrons have a tendency to tunnel into the side dot with increasing interdot hopping, which results in interference destruction between two transport channels. Further, this system exhibits a finite thermal response when a small thermal biasing (ΔT) is applied across the superconducting leads. The quasi-particle current flows across the junction due to thermal biasing, while the Josephson current is almost insensitive to thermal biasing. With increasing thermal biasing, the quasi-particle current produces a finite shift in the magnitude of the total current. Also, the magnitude of the total current decreases with increasing interdot hopping because the equivalent level of quantum dots moves further away from the Fermi level and thus cooper pair tunneling is suppressed.

Finally, we investigate the influence of interdot hopping and quantum dot energy levels on the thermophase Seebeck coefficient (TPSC). The magnitude of TPSC (S_ϕ) decreases with increasing interdot hopping when the energy levels of the side dot (QD_2) lie above the Fermi level and increase when energy levels of the side dot (QD_2) lie below the Fermi level. In the later case, when energy levels lie below the Fermi level, the equivalent level ($\epsilon_{d_i} \pm t$) of the quantum dot moves towards the Fermi level. Thus, the cooper pair tunneling increases with interdot hopping, and quasi-particle current is completely compensated by the Josephson current and the magnitude of TPSC peaks is enhanced.

We believe that the results presented in this study can be tested experimentally with the advancement in nano-fabrication techniques. In this paper, we consider the uncorrelated quantum dots, and the effect of the Coulomb correlation will be explored in future work. The present study can also be extended to investigate the thermal transport properties in systems where double quantum dots are coupled with superconducting leads in series, and parallel geometry and also for multi-terminal configurations. The concept of thermophase effect in quantum dot-based Josephson junction can be useful for future low-temperature thermal applications [60, 61, 62, 63] and need further investigation.

Acknowledgments

The authors acknowledge the financial support from the research project DST-SER-1644-PHY 2021-22. Bhupendra Kumar also acknowledges the support from the Ministry of Education (MoE), India, in the form of a Ph.D. fellowship.

References

- [1] B. D. Josephson. Possible new effects in superconductive tunnelling. *Physics Letters*, 1:251–253, 7 1962.
- [2] Philip W Anderson. How josephson discovered his effect. *Phys. Today*, 23(11):23–29, 1970.
- [3] Leo P Kouwenhoven, DG Austing, and Seigo Tarucha. Few-electron quantum dots. *Reports on Progress in Physics*, 64(6):701, 2001.
- [4] Marc A. Kastner. Artificial atoms. *Physics Today*, 46, 1993.
- [5] AV Rozhkov and Daniel P Arovas. Josephson coupling through a magnetic impurity. *Physical review letters*, 82(13):2788, 1999.
- [6] E Vecino, A Martín-Rodero, and A Levy Yeyati. Josephson current through a correlated quantum level: Andreev states and π junction behavior. *Physical Review B*, 68(3):035105, 2003.
- [7] Mahn-Soo Choi, Minchul Lee, Kicheon Kang, and Wolfgang Belzig. Kondo effect and josephson current through a quantum dot between two superconductors. *Physical Review B*, 70(2):020502, 2004.
- [8] Jong Soo Lim and Mahn-Soo Choi. Andreev bound states in the kondo quantum dots coupled to superconducting leads. *Journal of Physics: Condensed Matter*, 20(41):415225, 2008.
- [9] Yu Zhu, Qing-feng Sun, and Tsung-han Lin. Andreev bound states and the π -junction transition in a superconductor/quantum-dot/superconductor system. *Journal of Physics: Condensed Matter*, 13(39):8783, 2001.
- [10] Christoph Karrasch, Akira Oguri, and Volker Meden. Josephson current through a single anderson impurity coupled to bcs leads. *Physical Review B*, 77(2):024517, 2008.

- [11] DY Vodolazov and FM Peeters. Superconducting rectifier based on the asymmetric surface barrier effect. *Physical Review B*, 72(17):172508, 2005.
- [12] Yasunari Tanuma, Yukio Tanaka, and Koichi Kusakabe. Josephson current through a nanoscale quantum dot contacted by conventional superconductors. *Physica E: Low-dimensional Systems and Nanostructures*, 40(2):257–260, 2007.
- [13] A Dhyani, BS Tewari, et al. Interplay of the single particle and josephson cooper pair tunneling on supercurrent across the superconducting quantum dot junction. *Physica E: Low-dimensional Systems and Nanostructures*, 42(2):162–166, 2009.
- [14] Jordan A Van Dam, Yuli V Nazarov, Erik PAM Bakkers, Silvano De Franceschi, and Leo P Kouwenhoven. Supercurrent reversal in quantum dots. *Nature*, 442(7103):667–670, 2006.
- [15] K Grove-Rasmussen, H Ingerslev Jørgensen, and PE Lindelof. Kondo resonance enhanced supercurrent in single wall carbon nanotube josephson junctions. *New Journal of Physics*, 9(5):124, 2007.
- [16] A Eichler, M Weiss, S Oberholzer, C Schönenberger, A Levy Yeyati, JC Cuevas, and A Martín-Rodero. Even-odd effect in andreev transport through a carbon nanotube quantum dot. *Physical review letters*, 99(12):126602, 2007.
- [17] Yulin Ma, Tianqi Cai, Xiyue Han, Yaowen Hu, Hongyi Zhang, Haiyan Wang, Luyan Sun, Yipu Song, and Luming Duan. Andreev bound states in a few-electron quantum dot coupled to superconductors. *Physical Review B*, 99(3):035413, 2019.
- [18] J-D Pillet, P Joyez, MF Goffman, et al. Tunneling spectroscopy of a single quantum dot coupled to a superconductor: From kondo ridge to andreev bound states. *Physical Review B*, 88(4):045101, 2013.
- [19] Eduardo JH Lee, Xiaocheng Jiang, Manuel Houzet, Ramón Aguado, Charles M Lieber, and Silvano De Franceschi. Spin-resolved andreev levels and parity crossings in hybrid superconductor–semiconductor nanostructures. *Nature nanotechnology*, 9(1):79–84, 2014.
- [20] R Delagrangé, R Weil, A Kasumov, M Ferrier, H Bouchiat, and R Deblock. $0-\pi$ quantum transition in a carbon nanotube josephson junction: Universal phase dependence and orbital degeneracy. *Physical Review B*, 93(19):195437, 2016.
- [21] DB Szombati, S Nadj-Perge, Diane Car, SR Plissard, EPAM Bakkers, and LP Kouwenhoven. Josephson ϕ_0 -junction in nanowire quantum dots. *Nature Physics*, 12(6):568–572, 2016.
- [22] Shu-guang Cheng and Qing-feng Sun. Josephson current transport through t-shaped double quantum dots. *Journal of Physics: Condensed Matter*, 20(50):505202, 2008.
- [23] Feng Chi and Shu-Shen Li. Current–voltage characteristics in strongly correlated double quantum dots. *Journal of applied physics*, 97(12):123704, 2005.
- [24] Yu Zhu, Qing-feng Sun, and Tsung-han Lin. Probing spin states of coupled quantum dots by a dc josephson current. *Physical Review B*, 66(8):085306, 2002.
- [25] Rosa López, Mahn-Soo Choi, and Ramón Aguado. Josephson current through a kondo molecule. *Physical Review B*, 75(4):045132, 2007.
- [26] Stephanie Droste, Sabine Andergassen, and Janine Splettstoesser. Josephson current through interacting double quantum dots with spin–orbit coupling. *Journal of Physics: Condensed Matter*, 24(41):415301, 2012.
- [27] Gagan Rajput, Rajendra Kumar, et al. Tunable josephson effect in hybrid parallel coupled double quantum dot–superconductor tunnel junction. *Superlattices and Microstructures*, 73:193–202, 2014.
- [28] Minchul Lee, Rosa López, Ramón Aguado, Mahn-Soo Choi, et al. Josephson current in strongly correlated double quantum dots. *Physical review letters*, 105(11):116803, 2010.

- [29] JC Estrada Saldaña, A Vekris, G Steffensen, R Žitko, P Krogstrup, J Paaske, K Grove-Rasmussen, and J Nygård. Supercurrent in a double quantum dot. *Physical review letters*, 121(25):257701, 2018.
- [30] Silvano De Franceschi, Leo Kouwenhoven, Christian Schönberger, and Wolfgang Wernsdorfer. Hybrid superconductor–quantum dot devices. *Nature nanotechnology*, 5(10):703–711, 2010.
- [31] A Martín-Rodero and A Levy Yeyati. Josephson and andreev transport through quantum dots. *Advances in Physics*, 60(6):899–958, 2011.
- [32] V Meden. The anderson–josephson quantum dot—a theory perspective. *Journal of Physics: Condensed Matter*, 31(16):163001, 2019.
- [33] Glen D Guttman, Benny Nathanson, Eshel Ben-Jacob, and David J Bergman. Thermoelectric and thermophase effects in josephson junctions. *Physical Review B*, 55(18):12691, 1997.
- [34] F Giazotto, JWA Robinson, JS Moodera, and FS Bergeret. Proposal for a phase-coherent thermoelectric transistor. *Applied Physics Letters*, 105(6):062602, 2014.
- [35] Maria José Martínez-Pérez, Antonio Fornieri, and Francesco Giazotto. Rectification of electronic heat current by a hybrid thermal diode. *Nature nanotechnology*, 10(4):303–307, 2015.
- [36] F Giazotto, TT Heikkilä, and FS Bergeret. Very large thermophase in ferromagnetic josephson junctions. *Physical review letters*, 114(6):067001, 2015.
- [37] G Marchegiani, P Virtanen, F Giazotto, and M Campisi. Self-oscillating josephson quantum heat engine. *Physical Review Applied*, 6(5):054014, 2016.
- [38] G Marchegiani, A Braggio, and F Giazotto. Phase-tunable thermoelectricity in a josephson junction. *Physical Review Research*, 2(4):043091, 2020.
- [39] Alexander G Bauer and Björn Sothmann. Phase-dependent transport in thermally driven superconducting single-electron transistors. *Physical Review B*, 104(19):195418, 2021.
- [40] Yaakov Kleorin, Yigal Meir, Francesco Giazotto, and Yonatan Dubi. Large tunable thermophase in superconductor–quantum dot–superconductor josephson junctions. *Scientific Reports*, 6(1):1–7, 2016.
- [41] Mathias Kamp and Björn Sothmann. Phase-dependent heat and charge transport through superconductor–quantum dot hybrids. *Physical Review B*, 99(4):045428, 2019.
- [42] M. Krawiec. Thermoelectric transport through a quantum dot coupled to a normal metal and bcs superconductor. *Acta Physica Polonica A*, 114, 2008.
- [43] Sun-Yong Hwang, Rosa López, and David Sánchez. Cross thermoelectric coupling in normal-superconductor quantum dots. *Physical Review B*, 91(10):104518, 2015.
- [44] Sachin Verma and Ajay Singh. Non-equilibrium thermoelectric transport across normal metal–quantum dot–superconductor hybrid system within the coulomb blockade regime. *Journal of Physics: Condensed Matter*, 34(15):155601, 2022.
- [45] Sun-Yong Hwang, David Sánchez, and Rosa López. A hybrid superconducting quantum dot acting as an efficient charge and spin seebeck diode. *New Journal of Physics*, 18(9):093024, 2016.
- [46] Sun-Yong Hwang, Rosa López, and David Sánchez. Large thermoelectric power and figure of merit in a ferromagnetic–quantum dot–superconducting device. *Physical Review B*, 94(5):054506, 2016.
- [47] Sun-Yong Hwang, David Sánchez, and Rosa López. Nonlinear electric and thermoelectric andreev transport through a hybrid quantum dot coupled to ferromagnetic and superconducting leads. *The European Physical Journal B*, 90(10):1–7, 2017.

- [48] Piotr Trocha and Józef Barnaś. Spin-dependent thermoelectric phenomena in a quantum dot attached to ferromagnetic and superconducting electrodes. *Physical Review B*, 95(16):165439, 2017.
- [49] Wei-Ping Xu, Yu-Ying Zhang, Qiang Wang, Zhi-Jian Li, and Yi-Hang Nie. Thermoelectric effects in triple quantum dots coupled to a normal and a superconducting leads. *Physics Letters A*, 380(7-8):958–964, 2016.
- [50] Hui Yao, Chao Zhang, Peng-bin Niu, Zhi-Jian Li, and Yi-Hang Nie. Enhancement of charge and spin seebeck effect in triple quantum dots coupling to ferromagnetic and superconducting electrodes. *Physics Letters A*, 382(44):3220–3229, 2018.
- [51] Karol Izydor Wysokiński. Thermoelectric transport in the three terminal quantum dot. *Journal of Physics: Condensed Matter*, 24(33):335303, 2012.
- [52] G Michałek, Marcin Urbaniak, BR Bułka, T Domański, and KI Wysokiński. Local and nonlocal thermopower in three-terminal nanostructures. *Physical Review B*, 93(23):235440, 2016.
- [53] Robert Hussein, Michele Governale, Sigmund Kohler, Wolfgang Belzig, Francesco Giazotto, and Alessandro Braggio. Nonlocal thermoelectricity in a cooper-pair splitter. *Physical Review B*, 99(7):075429, 2019.
- [54] Glen D Guttman, Benny Nathanson, Eshel Ben-Jacob, and David J Bergman. Phase-dependent thermal transport in josephson junctions. *Physical Review B*, 55(6):3849, 1997.
- [55] Hartmut Haug, Antti-Pekka Jauho, et al. *Quantum kinetics in transport and optics of semiconductors*, volume 2. Springer, Berlin, 2008.
- [56] Leonid V Keldysh et al. Diagram technique for nonequilibrium processes. *Sov. Phys. JETP*, 20(4):1018–1026, 1965.
- [57] Dmitrii Nikolaevich Zubarev. Double-time green functions in statistical physics. *Soviet Physics Uspekhi*, 3(3):320, 1960.
- [58] Yigal Meir and Ned S Wingreen. Landauer formula for the current through an interacting electron region. *Physical review letters*, 68(16):2512, 1992.
- [59] Kicheon Kang. Transport through an interacting quantum dot coupled to two superconducting leads. *Physical Review B*, 57(19):11891, 1998.
- [60] Francesco Giazotto, Tero T Heikkilä, Arttu Luukanen, Alexander M Savin, and Jukka P Pekola. Opportunities for mesoscopics in thermometry and refrigeration: Physics and applications. *Reviews of Modern Physics*, 78(1):217, 2006.
- [61] HT Quan, YD Wang, Yu-xi Liu, CP Sun, and Franco Nori. Maxwell’s demon assisted thermodynamic cycle in superconducting quantum circuits. *Physical review letters*, 97(18):180402, 2006.
- [62] MJ Martínez-Pérez, P Solinas, and F Giazotto. Coherent caloritronics in josephson-based nanocircuits. *Journal of Low Temperature Physics*, 175(5):813–837, 2014.
- [63] Antonio Fornieri, Christophe Blanc, Riccardo Bosisio, Sophie D’ambrosio, and Francesco Giazotto. Nanoscale phase engineering of thermal transport with a josephson heat modulator. *Nature nanotechnology*, 11(3):258–262, 2016.